Supporting Information

Hanington et al. 10.1073/pnas.1011242107

SI Materials and Methods

Live material and Experimental Treatments. M-line and BS-90 strain *Biomphalaria glabrata* snails, and *Schistosoma mansoni* and *Echinostoma paraensei* were maintained as previously described (1, 2).

***B. glabrata* Oligonucleotide-Based Microarray.** Each microarray experiment made use of a *B. glabrata* oligonucleotide array (3, 4).

Acquired resistance microarray experiment. The experiment comprised three groups of snails and took place over the course of 16 d. Snails in the first group were exposed to 15–20 irradiated (4,000 rad) *E. paraensei* miracidia. Irradiated miracidia still penetrate the snail and migrate to the heart, but do not develop and are attacked by the snail defense system. RNA was isolated from 15 snails at 0.5, 1, 2, 4, or 8 d postexposure (dpe). Snails in the second experimental group were similarly exposed to irradiated *E. paraensei* miracidia, and 8 d afterward, were challenged with normal, viable miracidia (15–20 miracidia per snail). RNA was isolated from 15 individuals in this group at 0.5, 1, 2, 4, or 8 d postchallenge. Snails in the final group were exposed only to viable *E. paraensei* miracidia at the same dose and time as snails of the second group received their challenge dose. RNA was collected from 15 snails at each time point of 0.5, 1, 2, 4, and 8 dpe. For each treatment and time point, 3 replicate RNA samples were generated, each consisting of RNA pooled from five snails. From these pooled RNA samples, array probes were generated as previously described (3, 4).

Strain resistance microarray experiment. Snails of the BS-90 strain of *B. glabrata* are resistant to *S. mansoni* (PR-1 strain) and susceptible to *E. paraensei*, whereas M-line snails are susceptible to both parasites. Snails of each strain were exposed to 15–20 miracidia each of one parasite or the other. For each of the four combinations, 15 snails were collected at 0.5, 1, 2, 4, and 8 dpe. For each combination and time point, three replicate RNA samples were generated, each consisting of RNA pooled from five snails. From these pooled RNA samples array probes were generated as previously described (3, 4).

Size resistance microarray experiment. Adult (12–20 mm) M-line *B. glabrata* are resistant to *E. paraensei.* Two groups of adult snails were included. The first served as unexposed controls, and RNA was collected from them at the beginning of the experiment. Snails in the second group were each exposed to 15–20 *E. paraensei* miracidia and RNA was collected from five snails at 0.5, 1, 2, 4, 8, or 16 dpe. RNA from each snail was used separately to probe the array (3, 4).

RNA Isolation. RNA was isolated from snails using TRIzol reagent (Invitrogen), and specific details regarding RNA processing and handling have been previously published (3, 4).

Generation of cDNA Probes and Microarray Hybridization. cDNA was generated from 1 μg isolated whole–snail-body RNA (3, 4). A universal reference RNA probe was also synthesized and used to normalize the data. cDNA samples underwent second strand synthesis and were purified and labeled using either Cy5 (experimental), or Cy3 (universal reference). Both experimental and reference probes were purified and incubated with the oligo array slides overnight at 45 °C. Following hybridization, slides were washed and scanned.

Microarray Scanning and Analysis. Microarray slides were scanned using a GenePix 4000B scanner (Axon Instruments) with Genepix Pro-6.0 (Molecular Devices) software (3, 4). Significance was determined using a 5% false-positive rate, and a ± 1.5 $\log_2$ or greater change in expression was considered significant. Microarray data were deposited in the Minimum Information About a Microarray Experiment-compliant GEO database (http://www.ncbi.nlm.nih.gov/projects/geo) under the accession numbers GSE21878, GSE21880, and GSE21881.

Quantitative RT-PCR Analysis. Microarray results were confirmed for select transcripts including FREP3 using quantitative RT-PCR, with primers and protocols previously published (4).

Assessment of FREP3 sequence diversity. Individual M line *B. glabrata* (6- to 8-mm diameter), unexposed, or 1, 2, 3, or 4 dpe to *E. paraensei* (20 miracidia/snail) were bled by cardiac puncture, and hemocyte concentration was determined with a hemocytometer. Hemolymph was diluted using sterile snail saline (5mM Hepes, 3.7 mM NaOH, 36 mM NaCl, 2 mM KCl, 2 mM $MgCl_2$-$2H_2O$, 4 mM $CaCl_2$-$2H_2O$) to aliquot 20–40 hemocytes/10 μL/well of PCR plates, and hemocytes were lysed (10′, 94 °C) to release DNA. Preliminary experiments indicated that this number of hemocytes yielded adequate template for reliable PCR amplification under standard PCR conditions. For four hemocyte subsets per snail, PCR was performed using Takara Primestar high-fidelity polymerase and FREP3 specific primers (5′-AGTCCAAAGGTGTTATTGCATATG-3′, 5′-CTTCATCGGTCTGATTTTTCACT-3′) to target exon 5 of the FREP3 gene. Resulting amplicons were shotgun cloned (TOPO zero blunt; Invitrogen), plasmids were extracted from 96 transformants and inserts were sequenced on both strands (using vector primers and ABI BigDye 3.1). Controls for polymerase error and template switching were performed as before (5) to confirm the fidelity of the experimental PCR and sequencing methods. Sequences were edited and aligned (Sequencher 4.10, Gene Codes) for comparison within hemocyte subsets, within and among individual snails. Unique sequences were identified by clustering analysis (100% identity). Sequences recovered at high frequency were designated as source sequences. Variant sequences were compared against source sequences for single nucleotide differences (point mutations) and for containing sequence derived from different source sequences (gene conversion). The occurrence of gene conversion in candidate sequences was further tested using Geneconv software (6).

Analysis of FREP3 Genomic Architecture Using BAC Libraries. Screening of the BB02 strain *B. glabrata* BAC library (7) with FREP gene subfamily-specific probes (27), indicated that BAC clone BAC BB_Ba 125N1 (124-kb genomic insert) contained multiple FREP-encoding sequences. BAC DNA was isolated (BacMax DNA purification kit, Epicentre Biotechnology), and insert fragments (generated by partial digestion with restriction enzymes or by targeted PCR) were cloned, sequenced and subjected to contig aligment. Computational sequence analysis was performed to identify FREP-encoding sequences and intron–exon boundaries, and to determine nucleotide sequence identity relative to FREP3.2 (AY028461).

BrdU Labeling. In situ labeling of *B. glabrata* hemocytes used the In situ FLUOS BrdU labeling kit (Roche). Approximately 5–15 μL (depending on snail body size) undiluted BrdU labeling reagent was injected into the hemocoel of the snail. Snails were bled 24 h after injection, and hemolymph was placed on microscope slides to allow hemocytes to adhere. One hour later, the cells were

washed three times using 1× PBS (PBS) (13.6 mM NaCl, 0.26 mM KCl, 1 mM Na_2HPO_4, 0.18 mM KH_2PO_4, pH 7.4) and then fixed for 1 h. Slides were washed three times in 1× PBS and digested in 1.25 μg/mL proteinase K for 10 min at 37 °C. Slides were then placed in 4 M HCl denaturation solution for 10 min, followed by three washes in 1× PBS, 5 min/wash. After confirming the pH of the slide solution was above 6.5, slides were incubated in the blocking buffer provided with the kit, for 10 min. Detection of BrdU was performed using the provided anti-BrdU antibody at a 1:100 dilution of blocking buffer. Incorporation of BrdU into newly generated cells was detected using the Zeiss AxioSkop 2 mot plus microscope. Images were acquired using the Axiocam HRc (Zeiss) and processed using the Axio Image software (Zeiss).

Generation of in Situ Hybridization FREP3 Probes. Probes for the in situ detection of FREP3 mRNA were generated using FREP3 specific primers (5′-AGTCCAAAGGTGTTATTGCATATG-3′, 5′-CTTCATCGGTCTGATTTTTCACT-3′) to amplify a conserved region of FREP3. This PCR amplicon was cloned in both directions into pET 2.1 TOPO TA plasmids (Invitrogen) containing a T7 promoter site. Using T7 RNA polymerase both an anti-sense (experimental) and a sense (control) probe were synthesized and labeled using a DIG RNA labeling kit (Roche). Synthesized probes were diluted to 200ng/mL in DIG easy hyb (Roche). Slides were prepared as stated above (BrdU labeling section) and treated with 1.25 μg/mL proteinase K for 10 min at 37 °C. Slides were washed three times in PBS and preincubated with DIG easy hyb (1 h, 68 °C). Slides were transferred into hybridization solution containing the denatured RNA probe for 12–16 h at 68 °C, washed twice for 20 min with 42 °C with 2× sodium-chloride sodium-citrate (SSC) (30 mM NaCl, 3 mM sodium citrate [HOC (COONa) (CH_2COONa) 2.2H_2O)], and then twice at RT for 20 min with 0.1× SSC. Slides were then incubated overnight, in the dark, at RT, with anti-DIG antibody conjugated to a fluorescent label (Roche) diluted 1:250 using 0.5% BSA dissolved in Tris-buffered saline (TBS) (13.6 mM NaCl, 0.26 mM KCl, 2.5 mM Tris base) (blocking buffer). Slides were washed in PBS 3× for 5 min each. Slides were then dried and visualized. Fluorescence was detected using the Zeiss AxioSkop 2 mot plus microscope, and images acquired and processed as described above. If needed, background fluorescence was quenched using trypan blue (making a 25% solution using 1× PBS)

Purification and Generation of Anti-FREP3 Polyclonal Antibody. Full-length cDNA of FREP3 from M line *B. glabrata* was cloned in pCR2.1 vector (Invitrogen). Two primers were used for generation of an expression insert that targets the specific FREP3-IgSF1 region (8); forward primer pETbF3Ig1F (5′ CAGGCTAGCGGTTCAGAACTTGTCATAGA 3′; *Nhe* I) and reverse primer pETbF3Ig1R (5′ GTCCTCGAGTAAAGCGGTCGAGTTTGTTT 3′; *Xho* I). The corresponding restriction enzyme sites are underlined. The expression vector pET23b(+) (Novagen) was used for construction of the expression vector. The purified PCR product was then ligated to the pET23b(+) vector (Novagen). The resultant construct contained a conventional six-histidine (6xHis) sequence at the C terminus. The expression vector was transformed into the *Escherichia coli* BL21(DE3) strain (Novagen). Expression was induced with 0.7 mM IPTG (isopropyl-β-1-D-thiogalactopyranoside) for 6 h at 37 °C. Protein expression was confirmed by Western blot using an anti-6xHis monoclonal Ab. The C-terminal 6xHis tagged expressed polypeptide was purified using Ni-NTA agarose (Qiagen). Purified protein was sent to YenZym Antibodies, LLC (San Francisco, CA) for generation of antibodies in rabbits. The antibody was purified using the Protein A IgG purification kit (Thermo).

Analysis of FREP3 Antibody Localization by Fluorescence Microscopy. The FREP3 polyclonal antibody was used to detect FREP3 in cells prepared for the BrdU and in situ hybridization protocols described above. Colabeling studies attempting both antibody binding and in situ detection of FREP3 worked best in conjunction with the in situ hyridization protocol, in the following manner: BrdU nuclear staining (rhodamine conjugated antibody to BrdU (Roche), FREP3 mRNA (mouse antidioxigenin (1:100 dilution; incubated overnight at 37 °C), goat anti-mouse Alexa Fluor 637 (1:1,000 dilution; incubated at room temp for 4 h; Invitrogen), and the FREP3 protein using the anti-FREP3 (1:25 dilution; incubated at 37 °C overnight) antibody detected using a goat anti-rabbit fluorecein antibody (1:1,000 dilution; incubated for 4 h at room temperature) (Roche). Preparations were visualized in 1× PBS with 25% trypan blue to quench autofluorescence. Images were acquired and processed as above.

Immunoaffinity purification of FREP3 using the anti-FREP3 antibody. Rabbit anti-FREP3 antibody was conjugated to protein A-coated beads to generate a FREP3 immunoaffinity column using the Pierce Crosslink IP kit (Thermo Scientific). A 1-mL quantity cell-free *B. glabrata* plasma was incubated with the anti-FREP3 resin overnight at 4 °C. This process was repeated five times with new snail plasma to accumulate a significant quantity of FREP3 for functional studies. FREP3 was eluted according to the manufacturer's protocol and the eluant was assayed for purity (Silver stain plus; BioRad), and quantity (Nanodrop spectrophotometer; Thermo Scientific).

Biotinylation of Purified FREP3. Immunoaffinity purified FREP3 was biotinylated using the EZ-link Sulfu-NHS-Biotinylation Kit (Thermo Scientific). Success of the biotinylation reaction was measured using the Pierce Biotin Quantitation Kit (Thermo Scientific).

Conjugation of Biotinylated Monosaccharides and FREP3 to Streptavidin Microspheres. Biotinylated FREP3, α-D-mannose, *N*-acetylgalactosamine (GalNAc), α-D-galactose, α-D-glucose, *N*-acetylglucosamine (GlcNAc), α-L-fucose, and a biotinylation linker control (all monosaccharides and the linker control were produced by Glycotech) were all conjugated to fluorescent (YG) streptavidin-coated microspheres (Bang Laboratories). Briefly, microspheres were washed in PBS/BSA binding buffer three times, after which, they were incubated with biotinylated molecules for 2 h at 4 °C. Biotinylated FREP3 (30 μg) and biotinylated monosaccharides (50 μg) were incubated with 5×10^8 microspheres. The microspheres were centrifuged at 10,000 × *g* for 5 min and resuspended and washed three times in PBS/BSA binding buffer provided with the microspheres, then washed once and suspended in 1× PBS (pH 7.4), final concentration 2.5×10^6 microspheres per 10 μL, and used for injection or binding studies.

Injection of *B. glabrata* with Conjugated Microspheres. A 200-μL micropipette tip was modified to allow attachment of a 27-gauge needle to a 2–20 μL micropipettor (Nichipet EX). Using this apparatus, it was possible to uptake 10 μL biotinylated microsphere mixture. This and all other injections of snails were through the shell into the hemolymph sinus posterior to the albumin gland on the left side of the snail. Back bleeding was minimal if the needle was held in position for ∼15 seconds and then removed gently, and no microspheres were observed in the hemolymph that escaped through the injection site. Snails with 12- to 20-mm shell diameter were used. Release of microspheres into the snail hemocoel was observed to confirm successfull delivery.

Assessment of Phagocytosis by *B. glabrata* Hemocytes. In vivo phagocytosis of biotinylated and control microspheres was assessed in hemocytes isolated from snail hemolymph 2 h after

injection. Hemolymph was obtained by the head-foot retraction method (9) and placed on microscope slides for 1 h to allow the cells to adhere. The slides were then gently washed 3× in 1× PBS to remove any unphagocytosed microspheres. Fluorescence microscopy was used to observe the yellow fluorescing microspheres within hemocytes. To count only those microspheres that were truly phagocytosed and not simply bound on the surface of the cells only one focal plane was used to count from. For each treatment (FREP3 and all monosaccharides), as well as controls (unlabeled microspheres and the biotinylation linkage control conjugated microspheres), a total of six individual snails were used, divided into two separate experiments. For each snail, 100 hemocytes were inspected for the presence or absence of beads as well as the number of phagocytosed beads.

Assessment of FREP3 Binding to Monosaccharide-Coated Microspheres. Monosaccharide-coated microspheres were incubated with hemocyte-free snail plasma pooled from 10 individual uninfected M-line snails (10–15 mm in diameter). Approximately 5×10^8 monosaccharide-coated microspheres were incubated with 1 mL plasma. The incubation took place at 4 °C overnight, after which, the microspheres were washed three times in 1× PBS and then mixed with SDS/PAGE sample loading buffer containing 0.5% β-mercaptoethanol. A 30-μL quantity of the microsphere mixture was loaded onto an 8% SDS gel, which was transferred to a nitrocellulose membrane after it was run. The Western blot was blocked using 0.5% BSA in Tween-Tris-buffered saline (TTBS; TBS with 0.1% Tween 20) for 1 h and incubated at room temperature overnight in anti-FREP3 antibody (1:2,500 dilution). The blot was washed 3×, 10 min each, in 1× TTBS and then incubated in anti-rabbit-AP–conjugated antibody (Sigma) (1:5,000 dilution) for 2 h at room temperature. The blot was washed three times for 10 min each in 1× TTBS, and then three times for 10 min each in 1× TBS before being developed using NBT/BCIP development solution (Roche).

Design and Functional Assessment of FREP3-Specific siRNAs. FREP3-specific siRNA oligos were designed to target conserved sequence regions of FREP3 using the RNAi SciTools Web site (http://www.idtdna.com/Scitools/Applications/RNAi/RNAi.aspx?source=menu) from Integrated DNA Technologies (IDT). In total, four oligos were generated (CAGGUCUAGUGUUUGUACCAAUGAAGUACAAACACU, ACCACCACACGCUCGUCUACAGUACAGACGAGCGUG, AAAUCCAAGUCUUUGUUGAGAACAUCAACAAAGACU, GCUGUCUGAGAGAUCAUCCAAGAAAGAUGAUCUCUC) and used in knock-down experiments. The oligos were resuspended as suggested by the manufacturer (IDT), and 10 μL containing 200 μg pooled siRNas was injected into individual snails with the same technique used for microspheres. To confirm successful knock-down of FREP3, hemocytes were isolated from hemolymph bled from large (20- to 25-mm diameter) snails at 12, 24, 48, 72, 96, and 120 h post-injection. These cells were used as a template for RT-PCR, and the expression of FREP3 (5′-AGTCCAAAGGTGTTATTGCATATG-3′, 5′-CTTCATCGGTCTGATTTTTCACT-3′) was monitored in comparison with EF-α (5′-GACTGTGCAGTGCTGATTGTTGCT-3′, 5′-CAATCAAGCACAGGCGCATAACCA-3′) endogenous controls. Further confirmation of FREP3 knock-down at protein level was achieved by isolating plasma from snails before and then 4 d after siRNA injection. Plasma samples were diluted 1/10, separated by SDS/PAGE, and transfered to nitrocellulose. Blots were probed for the presence of FREP3 using the protocol described above. To control for nonspecific knock-down, GFP-specific siRNAs were designed (CCAUCAUCUUUGAAGAAGGAACAAUCUUCUUCAAAG, AGGUAAUAAUACAGGACCCGGUGAUGGUCCUGUAUU, AUGUUGUUACUAAUGUAGCCUUGACCUACAUUAGUA) and introduced into the snails using the same protocol. A 100-μg quantity of plasma protein, quantitated using the BCA protein quantitation kit (Thermo Scientific), was loaded into each well to control for protein amounts.

Breakdown of FREP3 Size Resistance Phenotype Using FREP3-Specific RNA Interference. In two separate trials, using the above RNAi protocol, adult *B. glabrata* M-line snails (12- to 20-mm diameter), which are resistant to infection with *E. paraensei*, were injected with either FREP3-specific siRNA oligos specified above or GFP-specific siRNA oligos to serve as controls. Following injection, all snails were exposed to 15–20 *E. paraensei* miracidia. Two weeks later, snails were dissected and the presence of *E. paraensei* redia stages was quantitated. Small infection sized *B. glabrata* (4- to 8-mm diameter) snails served as infection controls to confirm the viability of the parasites (>90% infection prevalence was observed in this group).

1. Loker ES, Cimino DF, Stryker GA, Hertel LA (1987) The effect of size of M line *Biomphalaria glabrata* on the course of development of *Echinostoma paraensei*. *J Parasitol* 73: 1090–1098.
2. Loker ES, Bayne CJ (1982) In vitro encounters between *Schistosoma mansoni* primary sporocysts and hemolymph components of susceptible and resistant strains of *Biomphalaria glabrata*. *Am J Trop Med Hyg* 31:999–1005.
3. Adema CM, et al. (2010) Differential transcriptomic responses of *Biomphalaria glabrata* (Gastropoda, Mollusca) to bacteria and metazoan parasites, *Schistosoma mansoni* and *Echinostoma paraensei* (Digenea, Platyhelminthes). *Mol Immunol* 47:849–860.
4. Hanington PC, Lun CM, Adema CM, Loker ES (2010) Time series analysis of the transcriptional responses of *Biomphalaria glabrata* throughout the course of intramolluscan development of *Schistosoma mansoni* and *Echinostoma paraensei*. *Int J Parasitol* 40:819–831.
5. Zhang SM, Adema CM, Kepler TB, Loker ES (2004) Diversification of Ig superfamily genes in an invertebrate. *Science* 305:251–254.
6. Sawyer S (1989) Statistical tests for detecting gene conversion. *Mol Biol Evol* 6: 526–538.
7. Adema CM, et al. (2006) A bacterial artificial chromosome library for *Biomphalaria glabrata*, intermediate snail host of *Schistosoma mansoni*. *Mem Inst Oswaldo Cruz* 101 (Suppl 1):167–177.
8. Zhang SM, Léonard PM, Adema CM, Loker ES (2001) Parasite-responsive IgSF members in the snail *Biomphalaria glabrata*: Characterization of novel genes with tandemly arranged IgSF domains and a fibrinogen domain. *Immunogenetics* 53:684–694.
9. Sminia, T, Barendsen L (1980) A comparative morphological and enzyme histochemical study on blood cells of the freshwater snails *Lymnaea stagnalis*, *Biomphalaria glabrata*, and *Bulinus truncatus*. *J Morphol* 165–31–39.

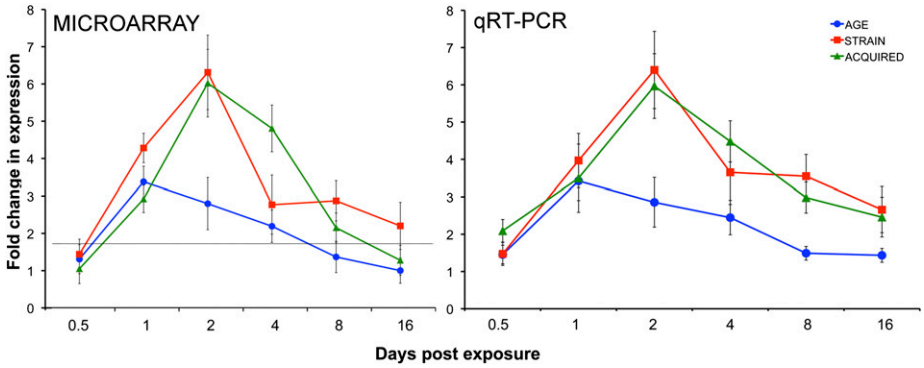

Fig. S1. Microarray and qRT-PCR expression profiles for FREP3, for three models of snail resistance to trematode infection (age, strain, and acquired resistance). Microarray values summarize FREP3 expression profiles, with data for each time point represented by a mean of triplicate samples, each sample derived from a pool of five snails. qRT-PCR values represent mean values of FREP3 expression from eight individual snails at each time point. Bars represent SE.

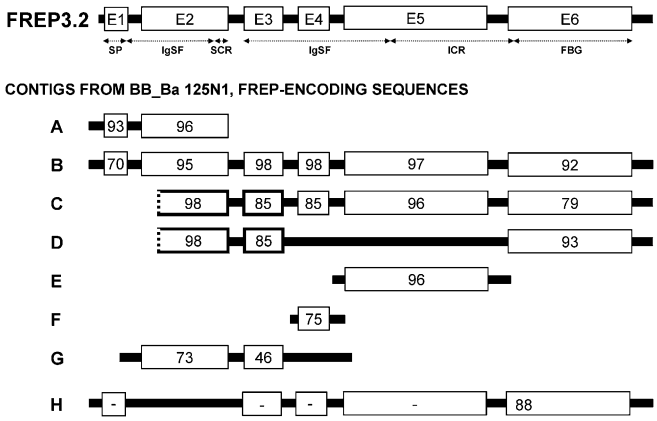

Fig. S2. FREP-encoding sequences (complete and partial genes) with high similarity to FREP3, cluster within the ~110-kbp insert of BAC clone BB_Ba 125N1. (*Upper*) The exon–intron structure of FREP3.2 (GenBank accession no. AY028461), not to scale (black lines = contiguous noncoding sequence; E1= exon 1, etc). The protein domains of FREP3.2 (double-headed arrows) are aligned with the gene structure. FBG, fibrinogen; ICR, interceding region; IgSF, Ig superfamily domain; SCR, short connecting region; SP, signal peptide. Analysis of sequence reads (NCBI trace archive gnl|ti|2278068446-2278071234) from the BAC clone yielded several unconnected contigs. Sequencing of the BAC clone yielded several unconnected contigs. Contigs A–E show exon–intron structures of sequences of the FREP3 gene subfamily (≥85% overall nt sequence identity). Bold lines denote exons with identical sequences shared by contigs C and D. Sequence identity of exons from contigs to those of FREP3.2 is indicated by numbers, (–) no relevant similarity. Many of these regions have nucleotide identity in excess of 90% which is conducive for the likelihood of gene conversion. Contigs F–H show additional FREP-encoding sequences assigned to other FREP gene subfamilies, with lower sequence identity percentages. The 3′ exon of contig H (belongs to FREP14 subfamily) has a region (residues 48–274 of 655 nt) that shares 88% nt identity with the FBG sequence of exon 6 of FREP3.2. Dotted lines indicate that exon sequencing is not complete.

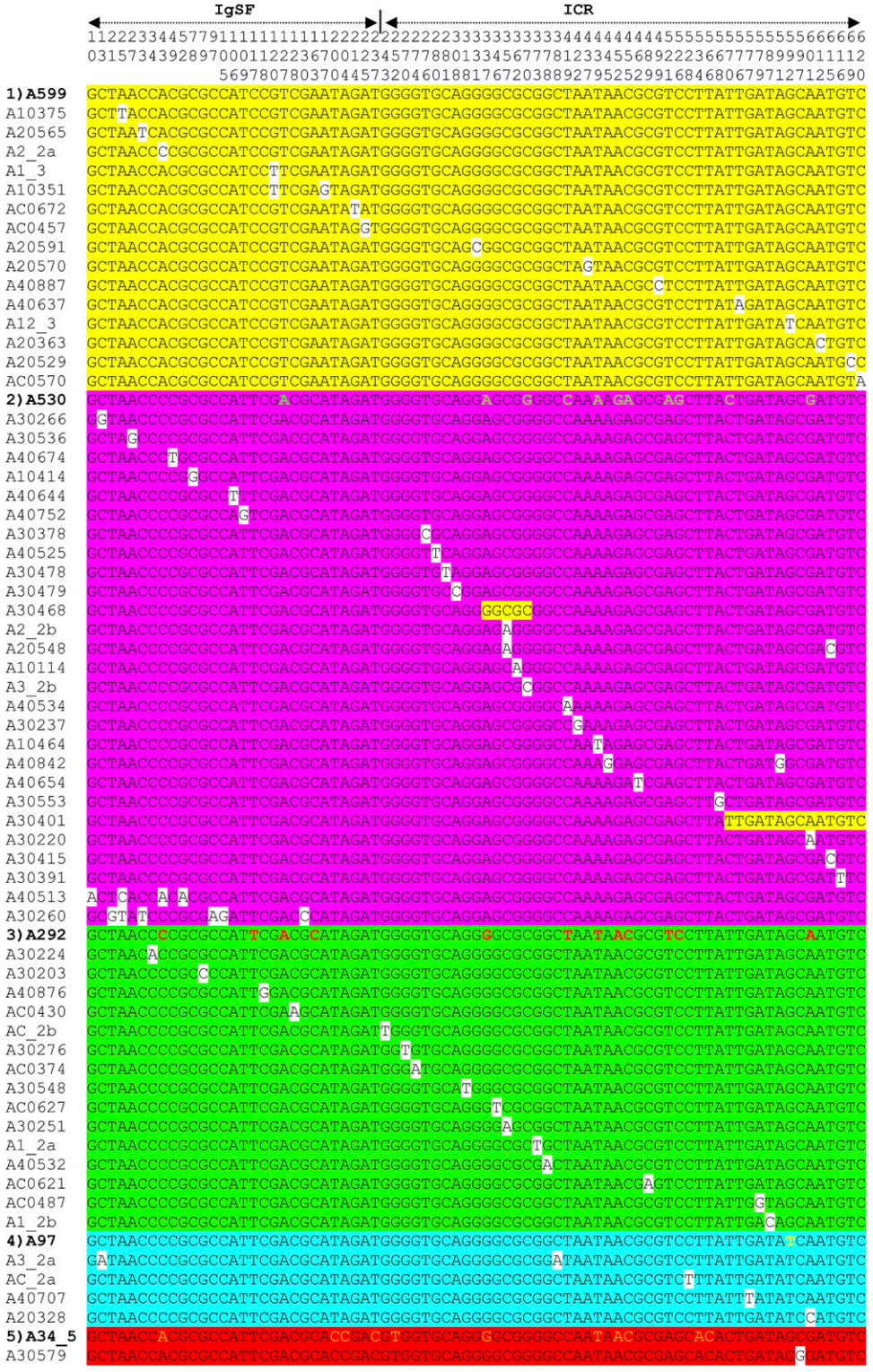

Fig. S3. Alignment of sequence variants of exon 5 of FREP3 derived from four hemocyte subsets (20–40 cells each) from each of five M line snails, diversification of source sequences by point mutation and gene conversion. Five sequences (A599, A292, A97, A530, A35_5; numbered, bold font) were recovered from genomic DNA of hemocytes at high frequency. These sequences (at the top of each of the five colored blocks) were designated as source sequences. Of the 626 base pairs sequenced, this alignment shows only the 77 variable nucleotide positions (top numbers); double-headed arrows indicate sequence intervals of exon 5 that encode the Ig superfamily domain (IgSF) and interceding region (ICR). Colored letters within the source sequences identify nucleotide differences to the above source sequence. Other sequence variants, recovered only once or at low frequency, have the same color as the source sequence that they are most similar to, single nucleotide differences (point mutations) are indicated by a white background. Geneconv software analysis provided statistically significant support for occurrence of two gene conversions; sequence A30401 ($P = 0.0089$) and A30468 ($P = 0.05$); different colors identify the sequence regions contributed by distinct source sequences. These are the putative gene conversions indicated in Fig. 2*B*.

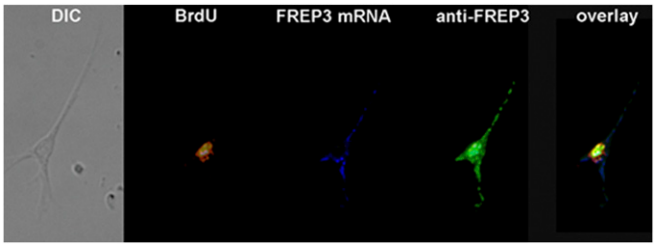

Fig. S4. Representative in situ hybridization photographs showing incorporation of BrdU into a newly generated hemocyte. This same hemocyte, originally photographed with differential interference contrast microscopy (DIC), is also colabeled for FREP3 mRNA (blue) and FREP3 protein expression (green). Overlay of all three fluorescent images is also shown.

Table S1. Transcripts up-regulated in *S. mansoni*-resistant BS-90 strain *B. glabrata* snails compared with control M-line snails after challenge with *S. mansoni*

	Days postexposure						
Transcripts up-regulated due to strain resistance	0.5	1	2	4	8	16	32
FREP10							7.40
FREP11	10.33		2.52	3.76			
FREP13		4.77					
FREP2	10.90	5.83	4.54	4.81	4.92	6.50	
FREP3		4.28	6.32	2.76	2.86	2.19	
FREP4	4.75	8.76	4.76	6.15	3.53	3.62	
FREP5		3.50					
FREP6		13.04	4.76	3.99	5.39	5.99	
FREP8		4.31	2.57	2.57	7.79		
Cadherin EGF	5.09	2.69	2.55		4.78	4.50	
Chorion peroxidase			5.21				
Coagulation factor XI		4.20					
Complement C1q TNF-related protein 3	12.47		8.57				
Complement C1q-like protein	2.57	5.27	7.04	5.40			
Dermatopontin	8.05	2.95	3.40	3.82	5.07	3.44	
Dermatopontin TRAMP		3.14	2.83				
Dual oxidase	10.74	5.50	8.81	8.15	13.51	4.61	
Epidermal growth factor-related prot			3.43	2.97	4.48		
FReD FREP2-like			2.21	1.90			
Galectin-4			7.24	8.85	6.90	4.68	
Galectin-7				2.11	6.80	3.83	
Galectin-9 A		2.99					
Heat shock 70 kDa protein 2	8.86	2.21					
Hemagglutinin/proteinase		3.21					
Histone H2A	8.84	3.98	7.34	4.29	6.65	5.83	
Histone H2AV H2A.F/Z	3.75	2.07	6.63	9.45			
Histone H3.3	7.50	3.70	9.00	7.07	7.39		
Lipopolysaccharide-binding prot LBP		2.81					
Macrophage migration inhibit factor BmMIF	9.82		3.77	3.40	3.17	3.75	
Macrophage expressed protein			4.05	3.12			
Macrophage mannose receptor 1 MMR			2.14	4.18			
MAP kinase 2	4.15						
Mitogen-activated prot kinase-binding Mp1			2.44	9.25			
Multidrug resistance protein 2			2.57				6.34
Multiple EGF-like domain protein 3					3.55	3.14	
NF-kappa-B p105 subunit			2.54				
Plectin-1			2.98	2.64	6.82	3.38	
Profilin-2			4.23	9.71			
Ras-related protein Rab5			1.92				
Ras-related protein Rap-1b		3.18					
Serine/threonine-protein kinase DCAMKL1			1.94				
Serine/threonine-protein kinase WNK1					1.94		
Superoxide dismutase 1 copper chaperone			6.59	8.00			
Superoxide dismutase Cu-Zn B		4.40	8.25	9.15	4.66	7.26	

Table S2. Transcripts up-regulated in large (>12-mm diameter) M-line snails compared with infection size (4- to 10-mm diameter) M-line snails after challenge to *E. paraensei*

	Days postexposure					
Transcripts up-regulated due to size resistance	0.5	1	2	4	8	16
Serpin peptidase inhibitor	8.13	9.60		31.33		9.42
Autophagy-related protein 3	4.60		1.73			
β-glucan recognition protein	1.51	1.74	1.56		1.50	
LBP/DPI	1.69	1.51	2.51	3.62	1.95	
FREP13	7.84	7.93	9.02	13.16	7.68	6.87
FREP3		3.37	2.79	2.18		
FREP4	2.33					
FREP9	2.20	2.00	1.59		1.76	
Chorion peroxidase precursor		12.00				
Dermatopontin	1.77	1.77	2.24		1.82	1.98
DSC-2	2.89	2.35	3.32	5.55	2.53	2.37
Epidermal growth factor-related protein	3.83					
FREM A	3.40		1.60	1.74	1.68	
Galectin-9 B	2.32	1.74	1.50		1.85	
G protein coupled receptor GRL101				2.67		
Gram-negative bacteria binding protein	1.81					
Heat shock 70 kDa protein	3.40	2.14				
Heat shock 70 kDa protein	1.79					
Heat shock protein 90	8.61					
Heat shock protein HSP 90-alpha A	1.76	7.77	9.13	12.52		
Heat shock protein HSP 90-alpha B	2.30	2.26				
LPS binding protein-like protein	2.51	1.85	2.62	3.71		2.22
Macrophage migration inhibit factor					2.28	
Macrophage mannose receptor 1 MMR	1.86					
Multidrug resistance-associated protein	3.52	2.42	2.43	2.38		
NF-κ-B p105 subunit	3.96					
Peptidoglycan-recognition protein-SC2			1.99			
Profilin-2	1.61	3.04			1.85	
Serine protease hepsin	9.79	1.91	1.64	1.58		
STAT 5B	2.40	9.07	10.98	12.51	8.98	7.28
Stress-induced-phosphoprotein 1 STI1	7.44	2.28	1.97		1.71	1.68
TGF-β type I receptor	2.11	7.19	8.13	16.99		8.17
TNF receptor-associated factor 1		3.06	1.94	2.72	1.87	

Table S3. Transcripts up-regulated in M-line snails sensitized to irradiated *E. paraensei* miracidia before secondary challenge with viable *E. paraensei* miracidia

	Days postexposure				
Transcripts up-regulated due to acquired resistance	0.5	1	2	4	8
Aplysianin-A precursor	27.68	31.73	39.99	27.42	21.96
Apoptosis 1 inhibitor dIAP1				2.56	
LBP/DPI	2.52	2.56	3.19		
FREP3		2.91	6.03	4.81	2.14
FREP7				2.13	
Complement C1q-like protein	3.47	6.20	3.43	6.03	7.31
Dermatopontin	3.08	4.11	4.07	5.08	4.06
FREM A	2.25				
G protein-coupled receptor kinase 1	2.89		2.70	4.19	
G protein coupled receptor GRL101	2.78	3.13	3.10	2.87	
Gram-negative bacteria binding protein	7.99	9.54	11.22	13.35	14.68
Heat shock 70 kDa protein	2.63	2.64			
Heat shock 70 kDa protein	2.49	3.50	2.37	6.07	4.73
Heat shock protein 70	28.64	30.85	31.77	43.49	41.10
Heat shock protein 90	3.03	3.43	3.16	2.31	2.15
Hemocyanin G-type	84.77	84.59	86.76	84.93	101.12
Histone H2A			2.29		
Inhibitor of apoptosis protein HIAP2				2.45	
JNK-interacting protein 1		2.33	2.71		
JNK-interacting protein		2.80	3.08	3.30	3.81
LPS- and beta-13-glucan-binding protein	2.97	2.64		2.44	
Matrilin-1 A					2.01
Matrilin-1 B	2.01				
Multiple EGF-like domain protein 3	2.03	3.15		2.39	3.11
Notch		2.49	2.39	3.17	3.54
Peptidoglycan-recognition protein-SC2		2.23			
Peroxidase precursor		2.26	3.47	5.80	5.41
Plectin-1	3.56	2.93	3.64	2.89	3.30
Serine/threonine-protein kinase 22A	3.35		2.64	2.28	
Serine/threonine-protein kinase Nek4	7.09	7.17	7.03	7.42	7.90
Serine-aspartate repeat-protein D			2.71		
Serpin B4	12.77	9.39	9.30	6.58	11.71
Serpin B6	4.17	4.81	3.46	4.80	5.96
SH3 domain-binding protein 5	2.91	3.34	3.19	2.60	
SH3-containing GRB2-like protein			2.62	2.81	
STAT 5B	11.81	25.35		21.22	
SMAD 4	2.06	2.27			2.62
Superoxide dismutase Cu-Zn	2.44	2.41	2.67		

Transcripts shown are those that were up-regulated in sensitized snails compared with normal M-line snails.